Fermi National Accelerator Laboratory

FERMILAB-Conf-91/300

Longitudinal Beam Dynamics at Transition Crossing

S.A. Bogacz

Fermi National Accelerator Laboratory
P.O. Box 500, Batavia, Illinois 60510

November 1991

* Presented at the *5th ICFA Beam Dynamics Workshop*, Corpus Christi, Texas, October 3-8, 1991.

Operated by Universities Research Association Inc. under Contract No. DE-AC02-76CHO3000 with the United States Department of Energy

Disclaimer

This report was prepared as an account of work sponsored by an agency of the United States Government. Neither the United States Government nor any agency thereof, nor any of their employees, makes any warranty, express or implied, or assumes any legal liability or responsibility for the accuracy, completeness, or usefullness of any information, apparatus, product, or process disclosed, or represents that its use would not infringe privately owned rights. Reference herein to any specific commercial product, process, or service by trade name, trademark, manufacturer, or otherwise, does not necessarily constitute or imply its endorsement, recommendation, or favoring by the United States Government or any agency thereof. The views and opinions of authors expressed herein do not necessarily state or reflect those of the United States Government or any agency thereof.

Longitudinal Beam Dynamics at Transition Crossing

S.A. Bogacz

Accelerator Physics Department, Fermi National Accelerator Laboratory*,

P.O. Box 500, Batavia, IL 60510, USA

Abstract

A brief outline of the longitudinal single particle dynamics at transition is presented in terms of phase-space mappings. Simple quantitative prediction about the phase-space dilution is made. More realistic simulation (ESME) of the transition crossing is carried out (including various collective and single particle effects contributing to the longitudinal emittance blow up). The simulation takes into account the longitudinal space-charge force (bunch length oscillation), the transverse space-charge (the Umstätter effect) and finally the dispersion of the momentum compaction factor (the Johnsen effect). As a result of this simulation one can separate relative strengths of the above mechanisms and study their individual effects on the longitudinal phase-space evolution, especially filamentation of the bunch and formation of a "galaxy-like" pattern.

1.0 Introduction

We start with a simple description of the longitudinal beam dynamics near transition. A pair of equations of motion is integrated analytically and expressed in terms of time evolution matrices and longitudinal phase-space trajectories. Mapping of equal density contours across transition yields quantitative predictions about the longitudinal emittance blow up. Our simple model does not include any nonlinearities nor intensity dependent forces. To illustrate more realistic phase-space dilution effects, we employ a tracking code ESME[1] (to simulate transition crossing in the Main Injector). One of the advantages of the simulation compared to existing analytic formalisms, e.g. based on the Vlasov equation[2], is that it allows us to consider the collective effects in a self-consistent manner with respect to the changing accelerating conditions. Furthermore, this scheme enables us to model nonlinearities of the longitudinal beam dynamics, which are usually not tractable analytically[3].

2.0 Single Particle Dynamics at Transition

The longitudinal motion, energy-phase oscillations (ε–ϕ), near transition is governed by the following set of equations

$$\frac{d\phi}{dt} = \eta \frac{h\omega_o}{E\beta^2}\varepsilon$$

and (1)

---

* Operated by the Universities Research Association under contract with the U.S. Department of Energy

$$\frac{d\varepsilon}{dt} = \frac{eV\omega_o}{2\pi} (\sin\phi - \sin\phi_s) \ ,$$

where the frequency slip factor, η, depends now on energy offset, ε, and also on time. It is given by the following expression

$$\eta = \alpha_o + (\alpha_o + 2\alpha_1 - \alpha_o^2) \frac{\varepsilon}{E\beta^2} - \frac{1}{\gamma_t^2} + \frac{eV\sin\phi_s\omega_o}{\pi E} t \ , \tag{2}$$

where ϕ_s is the synchronous phase. The momentum compaction factor,α , is defined by the following expansion

$$\frac{\Delta C}{C_o} = \alpha_o \ \delta + \alpha_1 \ \delta^2 + ... \ , \qquad \delta = \frac{\Delta p}{p_o} \ , \tag{3}$$

where C_o is the nominal closed orbit path length, and ΔC is the increase in path length for an off-momentum particle. The coefficients α_o and α_1 are geometrical properties of the lattice, given by

$$\alpha_o = \frac{2\pi}{C_o} \langle \chi_o \rangle \ , \quad \alpha_1 = \frac{2\pi}{C_o} \langle \chi_1 \rangle \ , \tag{4}$$

where angle brackets $\langle \ ... \ \rangle$ denote averaging weighted by bend angle. The quantities being averaged are component dispersions in a momentum expansion of the total dispersion function,χ ,given below

$$\chi = \chi_o \ \delta + \chi_1 \ \delta^2 + ... \ . \tag{5}$$

One can notice that the first and third terms in Eq.(2) cancel identically. To simplify these equations even more one introduces new set of canonical variables, θ–p, and dimensionless time in units of the nonadiabatic time, $\tau = t/T$, defined by

$$T = \sqrt[3]{\frac{2\pi}{h} \left(\frac{E}{eV}\right)^2 \frac{\gamma^2}{\beta} \frac{1}{\sin\phi_s |\cos\phi_s|}} \ . \tag{6}$$

The set of equations of motion in reduced variables simplifies as follows

$$\frac{d\theta}{d\tau} = (\tau + ap) \ p$$

and (7)

$$\frac{dp}{d\tau} = \frac{\sin(\phi_s + \theta) - \sin\phi_s}{|\cos\phi_s|} \ ,$$

where the coefficient

$$a = \frac{1}{2\alpha_o} (\alpha_1 + \frac{3}{2} \alpha_o) |\cot\phi_s| \ . \tag{8}$$

is proportional to the so-called Johnsen time, defined as the rms average of transition crossing time delay (with respect to the synchronous particle) taken over the entire bunch. The strength of this effect[7] is directly related to the formation of long tails and longitudinal emittance blow up. However, to reduce our model even more – to a minimum, but still nontrivial case of transition crossing – we turn this nonlinearity off for the time being, by setting a = 0. Applying linear approximation to the RF focussing in Eqs.(7) further reduces them to the second order Airy equation given below

$$\frac{d^2}{d\tau^2} p \pm \tau\, p = 0$$

and (9)

$$\theta \pm \frac{d}{d\tau} p = 0 \,.$$

Here the upper sign refers to 'above' and lower 'below' transition situations. A convenient way of illustrating solutions of this system of equation of motion is to introduce propagators for phase-space trajectories. A trajectory is defined in p–θ space by the following column vector

$$\underline{x}(\tau) = \begin{bmatrix} p(\tau) \\ \theta(\tau) \end{bmatrix} \,. \tag{10}$$

To propagate the above trajectory across transition one has to construct a time evolution matrix, **M**, for Eq.(9), defined according to

$$\underline{x}(\tau) = \mathbf{M}(\tau,-\tau)\, \underline{x}(-\tau) \quad , \tag{11}$$

where $\tau = 0$ was chosen at transition. Explicit form of the matrix **M** can be written in the following form

$$\mathbf{M}(\tau,-\tau) = \begin{bmatrix} 1 & 0 \\ 0 & -1 \end{bmatrix} \mathbf{A}(\tau) \begin{bmatrix} 0 & \sqrt{3} \\ \frac{1}{\sqrt{3}} & 0 \end{bmatrix} \mathbf{A}^{-1}(\tau) \quad , \tag{12}$$

where the matrix **A** is given below in terms of two orthogonal Airy functions Ai and Bi and their derivatives

$$\mathbf{A}(\tau) = \begin{bmatrix} \mathrm{Ai}(-\tau) & \mathrm{Bi}(-\tau) \\ \mathrm{Ai}'(-\tau) & \mathrm{Bi}'(-\tau) \end{bmatrix} \,. \tag{13}$$

The Airy functions are in turn expressed in terms of the Bessel functions of the first kind

$$\mathrm{Ai}(-\tau) = \frac{\sqrt{\tau}}{3} \left[J_{1/3}(\xi) + J_{-1/3}(\xi) \right] \quad ,$$

$$\mathrm{Bi}(-\tau) = \sqrt{\frac{\tau}{3}} \left[J_{-1/3}(\xi) - J_{1/3}(\xi) \right] \quad , \tag{14}$$

where

$$\xi = \frac{2}{3}\tau^{3/2} \ .$$

The mapping defined by **M** allows one to propagate any equal density contour across transition. Figure 1 illustrates evolution of initially elliptical contour. Since **M** represents a linear mapping the contour remains elliptical, but its area gets compressed approaching transition. After transition the area enclosed by the contour expands and the final contour represents the same longitudinal emittance as the initial one. The final ellipse is stretched and rotated with respect to the initial one. We can conclude qualitatively that when the kinematic nonlinearities are present ($a \neq 0$) shearing will filament the contour and it will gradually fill up the smallest matched (straight) ellipse, which includes the final contour in Figure 1. To get a qualitative result for a realistic situation, where both kinematic nonlinearities and intensity dependent forces are present, one resorts to numerical solution of the original set of equations of motion, where Johnsen effect and the space charge forces are built in explicitly. This will be carried out in the next section.

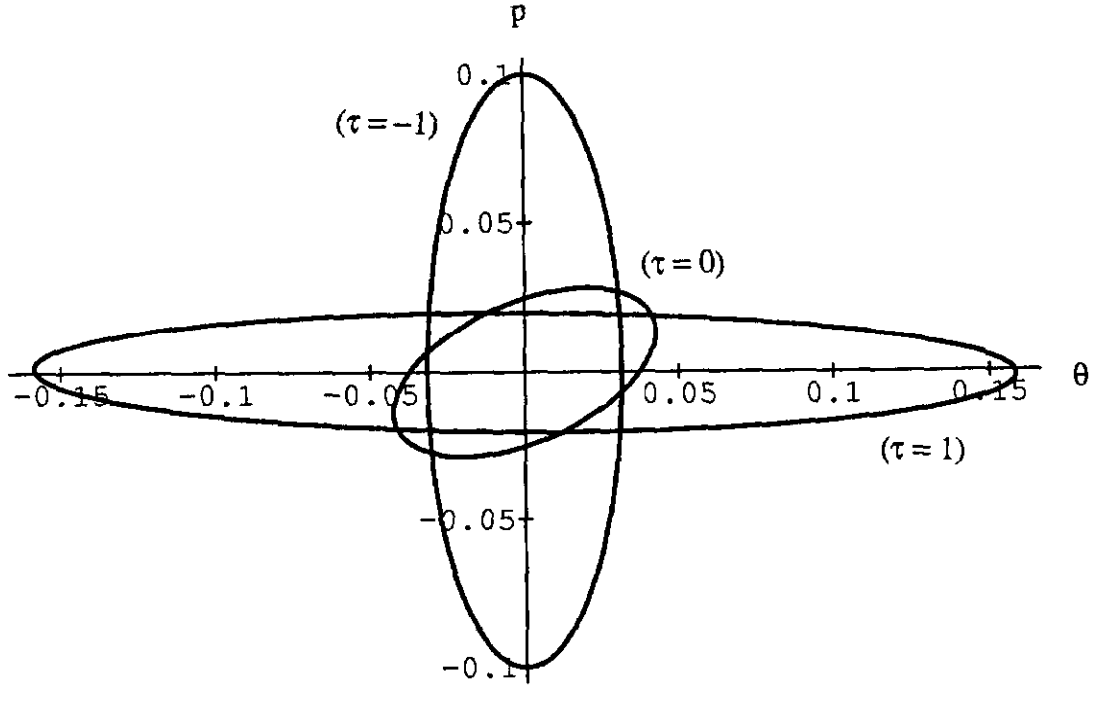

Figure 1: Equal density contours: below transition ($\tau = -1$), at transition ($\tau = 0$) and above transition ($\tau = 1$)

3.0 Longitudinal Phase Space Tracking with the Space Charge

The tracking procedure used in ESME consists of turn-by-turn iteration of a pair of Hamilton-like difference equations describing synchrotron oscillation in ϕ–ε phase-space ($0 \le \phi \le 2\pi$ for the whole ring and $\varepsilon = E - E_o$, where E_o is the synchronous particle energy). Knowing the particle distribution in the azimuthal direction, $\rho(\phi)$, and the revolution frequency, ω_o, after each turn, one can construct the longitudinal wake field induced by the coherent space charge force[4]

$$V_i(\phi) = e\omega_o \sum_{n=-\infty}^{\infty} \rho_n Z_{s\text{-}c}(n\omega_o) e^{in\phi},$$

where (15)

$$Z_{s\text{-}c}(n\omega_o) = \frac{nZ_o}{2\beta\gamma^2} \left\{ 1 + 2 \ln \frac{b}{a} \right\} .$$

Here, a and b are the radii of the beam and the smooth vacuum pipe, respectively.

The above force is defocusing below and focusing above the transition. Therefore it corrects the equilibrium bunch length to be longer below and shorter above the transition (compared to the case without any space charge). This yields bunch length oscillation above the transition set off by nonlinear bunch length overshoot[5].

4.0 Implementation of the Umstätter and Johnsen Effects

As a result of the transverse space charge forces each particle suffers a horizontal betatron tune shift, which is proportional to the particle density, $\rho(\phi)$, at the given longitudinal position ϕ. This tune shift translates directly into the change of γ_t. Close to the transition, when η goes through zero, even very small corrections to γ_t play dominant role and they govern the longitudinal beam dynamics. One of the features of ESME code is that each particle has its own γ_t, which allows for straightforward implementation of the Umstätter effect (described above). Similarly, to account for the dispersion of the momentum compaction factor (Johnsen effect), different parts of the bunch (particles with different momentum offset) are allowed to cross transition at different times. Both contributions to the γ_t shift are summarized below[6]

$$\Delta \left(\frac{1}{\gamma_t} \right)^2 = 2hr_p R \frac{1}{\beta^2\gamma^7 a^2} \rho(\phi) - (2\alpha_1 + \alpha_o - \alpha_o^2) \frac{\Delta p}{p} \quad . \tag{16}$$

5.0 ESME Simulation – Main Injector

As a starting point for our simulation a single bucket of the Fermilab Main Injector in ϕ–ε phase-space is populated with 5000 macro-particles according to a bi-Gaussian distribution matched to the bucket so that 95% of the beam is confined within the contour of the longitudinal emittance of 0.4 eV–

sec. Each macro-particle is assigned an effective charge to simulate a bunch intensity of 6×10^{10} protons.

The first set of results, Figure 2, corresponds to the situation when only intensity-dependent coherent forces are present ($\alpha_1 = 0$). The simulation is carried out over a symmetric (with respect to the transition) time interval of 2700 turns. Figure 2 represents a sequence of the longitudinal phase-space snapshots taken every 400 turns. One can clearly see dilution effects leading to extensive filamentation of the beam at transition. It yields the longitudinal emittance blowup (100%) and beam loss (5%) at transition.

The second set of simulations incorporates in addition to previously discussed coherent space charge forces also the Johnsen effect. The dispersion of the momentum compaction factor, α_1, is assigned a value of 5×10^{-3} and both the longitudinal and transverse space charge forces described by Eqs. (15) and (16) are used in the simulation. Again, the phase-space snap shots are illustrated in Figure 3. One can see fast development of long tails contributing to the longitudinal emittance blow up (150%) and substantial (30%) beam loss, since the particles from the tails quickly stream to the unstable phase-space region.

6.0 Conclusions

One can see from our simulation that the presence of large α_1 has crucial impact on beam degradation at transition. One can look at the Johnsen effect using simple physical picture of instantaneous phase-space configurations. Particles with large positive momentum offset cross transition sooner than the synchronous particle and they end up "seeing" unstable phase-space region long before the synchronous phase is "snapped" ($\phi_s \rightarrow \pi - \phi_s$ at the transition crossing for the synchronous particle). They follow unstable orbits in phase-space and eventually leave the bucket (long tail formation). Similarly, for particles with large negative momentum offset transition crossing is delayed with respect to the synchronous particle. After the synchronous phase "snap" they are still below transition and drifting into unstable region, which contributes to formation of the second tail (see Figures 2 and 3).

7.0 References

1. J.A. MacLachlan, FERMILAB TM-1274 (1984)
2. S. Krinsky and J.M. Wang, Particle Accelerators, **17**, 109 (1985)
3. S. Stahl and S.A. Bogacz, Phys. Rev. D, **37**, 1300 (1988)
4. J.A. MacLachlan, FERMILAB FN-446 (1987)
5. S.A. Bogacz and K-Y Ng, Phys. Rev. D, **36**, 1538 (1987)
6. A. Sørenssen, Particle Accelerators, **6**, 141 (1975)
7. S.A. Bogacz, Transition crossing in the Main Injector - ESME simulation, Proceedings of the F III Instability Workshop, Fermilab, July 1990.

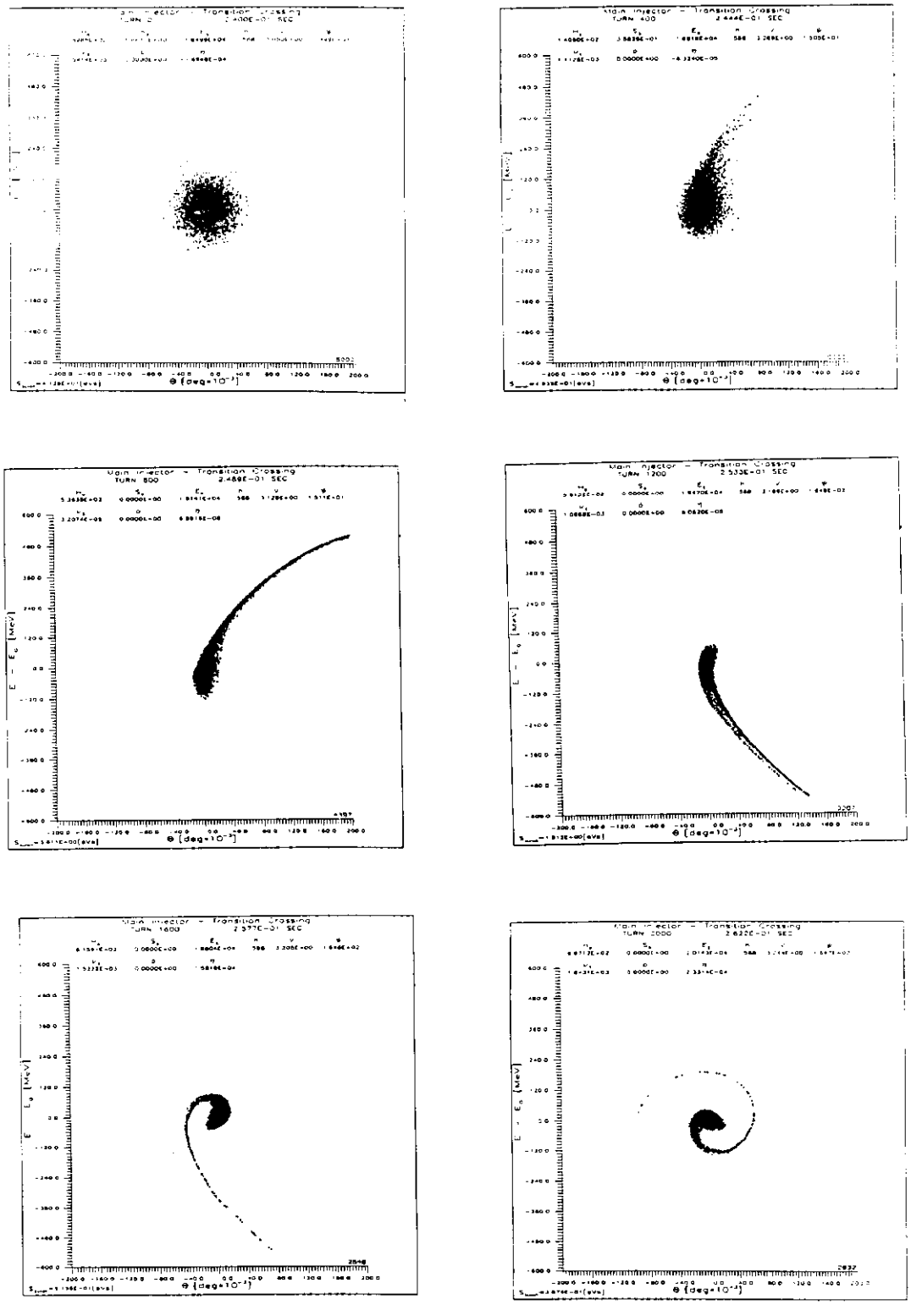

Figure 3: Phase-space dilution for ($\alpha_1 = 5\times10^{-3}$) illustrated by a sequence of the longitudinal phase-space snap-shots taken every 400 turns.

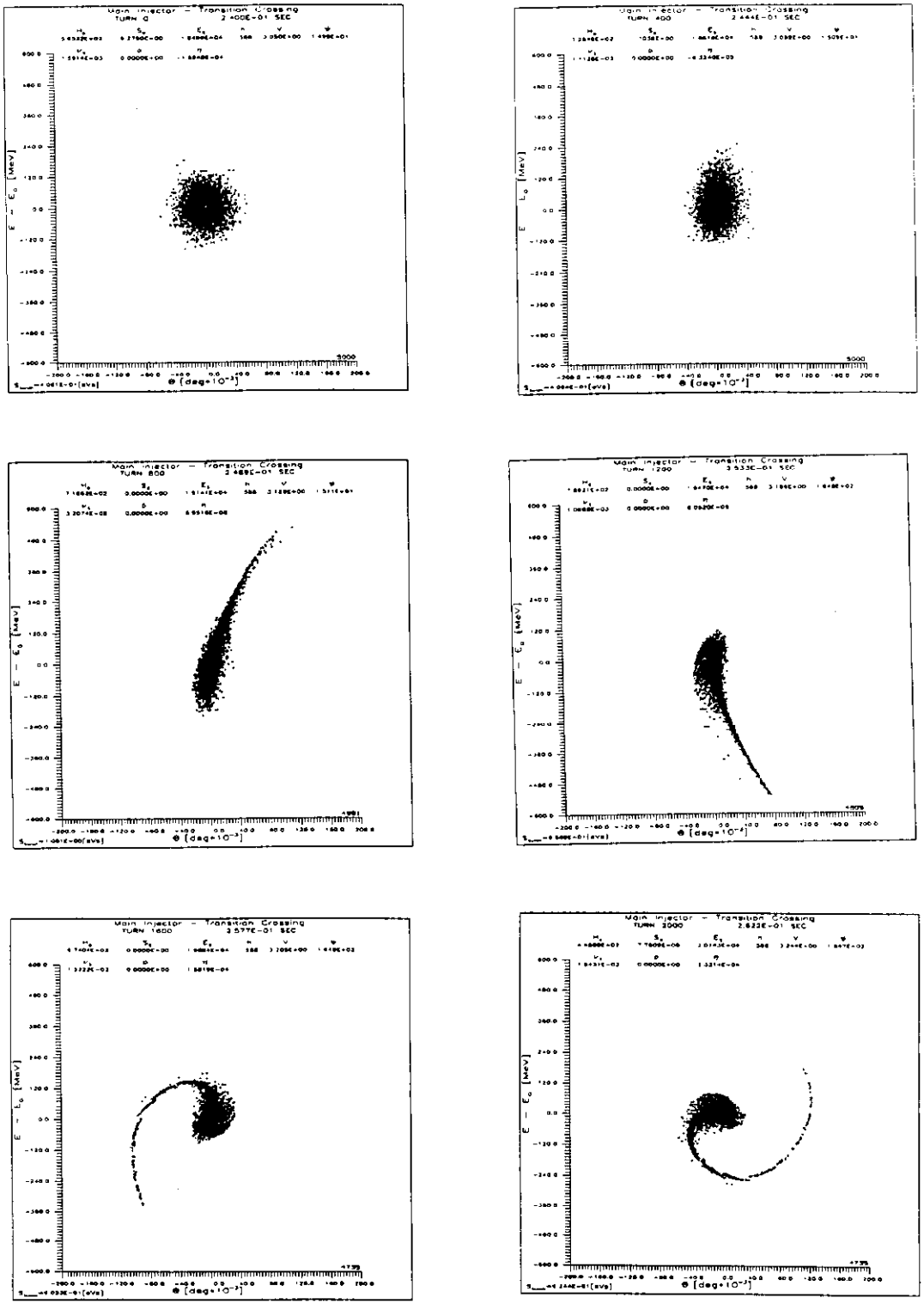

Figure 2: Phase-space dilution for ($\alpha_1 = 0$) illustrated by a sequence of the longitudinal phase-space snap-shots taken every 400 turns.